Hindawi
Mathematical Problems in Engineering
Volume 2019, Article ID 3914314, 10 pages
https://doi.org/10.1155/2019/3914314

Research Article

Training Sequence Design of TDS-OFDM Signal in Joint Radar and Communication System

Jiajun Zuo, Ruijuan Yang, Shaohua Luo, and Xiaobai Li

Department of Early Warning Intelligence, Air Force Early Warning Academy, Wuhan 430019, China

Correspondence should be addressed to Jiajun Zuo; zuojiajun59@126.com

Received 28 May 2019; Accepted 14 July 2019; Published 30 July 2019

Academic Editor: Paolo Addesso

In the joint radar and communication system, using orthogonal frequency division multiplexing (OFDM) signals, cyclic prefix (CP) and pilots lead to the problem of high peak at the sidelobe (PSL) level in autocorrelation function (ACF), which deteriorates the radar detection performance seriously. To solve this problem, first, a new RadCom signal based on time-domain synchronization OFDM (TDS-OFDM) was proposed. TDS-OFDM adopts training sequence (TS) for guard interval, as well as synchronization and channel estimation, so that CP and pilots can be avoided. And then, ambiguity function (AF) of TDS-OFDM RadCom signal was analyzed. Finally, TS are optimized to suppress PSL of TDS-OFDM signal and maintain the autocorrelation properties of TS simultaneously. The results show that the autocorrelation performance of designed TDS-OFDM RadCom signal is much better than that of CP-OFDM RadCom signal. Considering the importance of radar target detection, TDS-OFDM is more appropriate than CP-OFDM for the RadCom system.

1. Introduction

Joint radar and communication (RadCom) is proposed as a technology using a single signal to accomplish both radar and communication functions, which can not only effectively reduce the load of the platform, energy consumption, and electromagnetic interference, but also greatly improve the utilization of energy and spectrum, thus receiving much attention from military and civil fields [1–4].

Orthogonal frequency division multiplexing (OFDM) is a multicarrier data transmission technology which has been widely used in communication system. Due to the flexibility in waveform design, OFDM has also been gradually utilized in radar [5–7], thus becoming a suitable RadCom signal waveform. To improve data transmission rate, the pulse signal consisted of multiple OFDM symbols that were used in RadCom system [8–12]. To mitigate intersymbol interference (ISI), cyclic prefix (CP) of appropriate length has been used among OFDM symbols as guard interval (GI).

The application of CP suppresses the intercarrier interference (ICI) and improves the orthogonality of subcarriers. However, when CP-OFDM signal is utilized in the RadCom system, CP, the replication of the later section of OFDM data block, will inevitably cause the high level sidelobes of autocorrelation function (ACF). Moreover, the CP sidelobe level increases with the length ratio of CP and OFDM data block. In addition, to achieve communication synchronization and channel estimation, pilots must be used in CP-OFDM RadCom signal, but the pilot symbols will also lead to the problem of pilot sidelobes. Those sidelobes deteriorate the performance of radar target detection; thus the application of OFDM radar-communication integration will be severely restricted.

To address the problem, a solution is put forward in [13, 14]; that is, zero padding is performed for the CP and pilot tones of the reference signal before the correlation with echo signal. However, despite the effective elimination of the CP and pilot sidelobes, such approach will greatly deteriorate the target detection performance result of the decline of pulse gain caused by the loss of signal energy. In this paper, a new form of RadCom signal based on TDS-OFDM is proposed, where CP is replaced by training sequences (TS) as guard interval while being employed in communication synchronization and channel estimation. Accordingly, CP and pilot sidelobes can be avoided as neither cyclic prefix nor pilot tones is required.

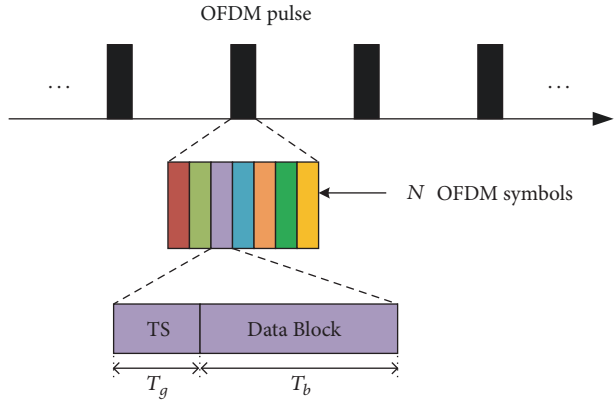

Figure 1: Structure of TDS-OFDM RadCom signals.

Being matured in communication, TDS-OFDM is a key technology in the standard of digital television terrestrial broadcasting (DTTB), whose application is successful in China, Cuba, Cambodia, etc. [15–17], so what is mainly studied in this paper is the performance of TDS-OFDM RadCom signal in radar application. Firstly, the ambiguity function (AF) of TDS-OFDM RadCom signal is deduced. And then, a TS design criterion is proposed, based on which, genetic algorithm is used to search optimal TS; finally, the TDS-OFDM RadCom signal with good performance both in radar and communication is generated.

The rest of the paper is organized as follows. The TDS-OFDM RadCom signal model is presented in Section 2 and the derivation of AF of TDS-OFDM RadCom waveform is described in Section 3. Then the optimization procedure and simulation results analysis of TDS-OFDM waveform follow in Sections 4 and 5. Finally, conclusions are drawn in Section 6.

2. Signal Model

As shown in Figure 1, designed TDS-OFDM RadCom system adopts pulse radar signal, where each pulse consists of N OFDM symbols. Each OFDM symbol is composed of a TS and an OFDM data block, with the duration of T_g and T_b, respectively. Then, the envelope of a TDS-OFDM RadCom pulse is presented as the sum of the following two parts:

$$s(t) = A_1 s_1(t) + A_2 s_2(t) \tag{1}$$

where $s_1(t)$ is the TS-string composed of N TS, $s_2(t)$ is the data blocks of N OFDM symbols, A_1 and A_2 are their amplitudes, respectively, and there is ${A_1}^2 + {A_2}^2 = 1$.

$$s_1(t) = \sum_{n=0}^{N-1} \sum_{k=0}^{K-1} c_{n,k} \mathrm{rect}\left(\frac{t - kT_1 - nT_2}{T_1}\right) \tag{2}$$

$$s_2(t) = \sum_{n=0}^{N-1} \sum_{m=0}^{M-1} d_{n,m} e^{j2\pi m\Delta f(t-nT_2-T_g)} \mathrm{rect}\left(\frac{t - nT_2 - T_g}{T_b}\right) \tag{3}$$

where $c_{n,k}$ is the nth code element of kth TS, which is assigned as $\pm c_0$ and satisfies the energy normalized condition of $\int |s_1(t)|^2 \mathrm{d}t = 1$. K is the number of code elements in a TS, $T_1 = T_g/K$ is the duration of a code element satisfying $T_1 = 1/B$, and B is the bandwidth of TDS-OFDM signal. $T_2 = T_g + T_b$ is the duration of a complete OFDM symbol, and rect(•) is the rectangular function. In (3), M is the number of subcarriers, Δf is the frequency interval between adjacent subcarriers, and $\Delta f = 1/T_b$ to keep the orthogonality of subcarriers. $d_{n,m}$ is the data transmitted on the mth subcarrier of the nth OFDM symbol, which can be modulated by phase shift keying (PSK) modulation or quadrature amplitude modulation (QAM). $d_{n,m}$ at different locations is independent and satisfies the expectation $\mathscr{E}[d_{n,m}] = 0$ and the energy normalized condition of $\mathscr{E}[\int |s_2(t)|^2 \mathrm{d}t] = 1$.

3. Derivation of Ambiguity Function

Ambiguity function demonstrates the delay-Doppler characteristics of the radar signal, making it an important tool for studying radar signal and waveform design. In this section, AF of TDS-OFDM RadCom signal is deduced in detail.

3.1. Ambiguity Function of TDS-OFDM RadCom Signal. For general point targets, the following narrowband AF can be used for analysis:

$$\chi(\tau, \xi) = \int_{-\infty}^{+\infty} s(t) s^*(t - \tau) e^{j2\pi\xi t} dt \tag{4}$$

where τ is time delay and ξ is Doppler shift. Substituting (1) into (4), AF of TDS-OFDM RadCom signal $\chi_s(\tau, \xi)$ can be derived

$$\begin{aligned} \chi_s(\tau, \xi) = {} & A_1^2 \chi_{1,1}(\tau, \xi) + A_2^2 \chi_{2,2}(\tau, \xi) \\ & + A_1 A_2 \chi_{1,2}(\tau, \xi) + A_1 A_2 \chi_{2,1}(\tau, \xi) \end{aligned} \tag{5}$$

where $\chi_{i,j}(\tau, \xi) = \int_{-\infty}^{+\infty} s_i(t) s_j^*(t - \tau) e^{j2\pi\xi t} dt$, $i, j = 1, 2$. $\chi_{1,1}(\tau, \xi)$ and $\chi_{2,2}(\tau, \xi)$ are the self-ambiguity functions of TS-string and OFDM data blocks, respectively; $\chi_{1,2}(\tau, \xi)$ and $\chi_{2,1}(\tau, \xi)$ are cross-ambiguity functions of TS-string and OFDM data blocks. Since $\mathscr{E}[d_{n,m}] = 0$, the expectation of

cross-ambiguity function $\mathscr{E}[\chi_{1,2}(\tau,\xi)] = \mathscr{E}[\chi_{2,1}(\tau,\xi)] = 0$. Thus, if we take the expected value of both sides of (5), there is the following.

$$\mathscr{E}\left[\chi_s(\tau,\xi)\right] = A_1^2\chi_{1,1}(\tau,\xi) + A_2^2\mathscr{E}\left[\chi_{2,2}(\tau,\xi)\right] \quad (6)$$

In fact, increasing the time-bandwidth product of OFDM pulse can effectively reduce the variance of $\chi_s(\tau,\xi)$ [18]. Thus, the following approximation is reasonable for the signal with high time-bandwidth product.

$$\chi_s(\tau,\xi) \approx \mathscr{E}\left[\chi_s(\tau,\xi)\right] \quad (7)$$

In addition, phase-coherent accumulation technology is generally used in modern radar, which can lower the variance of ACF further. Combining (6) and (7), $\chi_s(\tau,\xi)$ approximately equals the weighted sum of $\chi_{1,1}(\tau,\xi)$ and $\mathscr{E}[\chi_{2,2}(\tau,\xi)]$ about energy ratio. The following two subsections will derive these two AFs, respectively.

3.2. Ambiguity Function of OFDM Data Blocks. First, we deduce the AF of OFDM data blocks. According to the definition of AF, (4) can be represented as

$$\chi(\tau,\xi) = \int_{-\infty}^{+\infty} s\left(t+T_g\right)s^*\left(t+T_g-\tau\right)\mathrm{e}^{j2\pi\xi(t+T_g)}dt \quad (8)$$

and, substituting (3) into (8), AF of $s_2(t)$ is as follows.

$$\chi_{2,2}(\tau,\xi) = \sum_{n=0}^{N-1}\sum_{n'=0}^{N-1}\sum_{m=0}^{M-1}\sum_{m'=0}^{M-1}\left\{d_{n,m}d_{n',m'}^*\mathrm{e}^{j2\pi\Delta f(n'm'T_2-nmT_2+m'\tau)}\int_{-\infty}^{+\infty}\mathrm{e}^{j2\pi(m\Delta f-m'\Delta f+\xi)t}\mathrm{rect}\left(\frac{t-nT_2}{T_b}\right)\mathrm{rect}\left(\frac{t-n'T_2-\tau}{T_b}\right)dt\right\}\mathrm{e}^{j2\pi\xi T_g} \quad (9)$$

Let $F = m\Delta f - m'\Delta f + \xi$, and the integral term in (9) is as follows.

$$I = \int_{-\infty}^{+\infty}\mathrm{e}^{j2\pi Ft}\mathrm{rect}\left(\frac{t-nT_2}{T_b}\right)\mathrm{rect}\left(\frac{t-n'T_2-\tau}{T_b}\right)dt \quad (10)$$

The integral is discussed in two cases:

① when $(n-n')T_2 < \tau \le (n-n')T_2 + T_b$,

$$I = \int_{n'T_2+\tau}^{nT_2+T_b}\mathrm{e}^{j2\pi Ft}dt = \left(T_b + nT_2 - n'T_2 - \tau\right)\cdot\mathrm{e}^{j2\pi F(T_b+nT_2+n'T_2+\tau)}\mathrm{sinc}\left[F\left(T_b+nT_2-n'T_2-\tau\right)\right] \quad (11)$$

② when $(n-n')T_2 - T_b < \tau \le (n-n')T_2$,

$$I = \int_{nT_2}^{n'T_2+T_b+\tau}\mathrm{e}^{j2\pi Ft}dt = \left(T_b + n'T_2 - nT_2 + \tau\right)\cdot\mathrm{e}^{j2\pi F(T_b+nT_2+n'T_2+\tau)}\mathrm{sinc}\left[F\left(T_b+n'T_2-nT_2+\tau\right)\right] \quad (12)$$

and, combining (11) and (12), we can get the analytical expression of the integral as

$$I = \left(T_b - \left|nT_2 - n'T_2 - \tau\right|\right)\cdot\mathrm{e}^{j\pi F(T_b+nT_2+n'T_2+\tau)}\mathrm{sinc}\left[F\left(T_b-\left|nT_2-n'T_2-\tau\right|\right)\right], \quad (n-n')T_2 - T_b < \tau \le (n-n')T_2 + T_b \quad (13)$$

where $\mathrm{sinc}(x) = \sin(\pi x)/\pi x$. Substituting (12) into (9) yields the following.

$$\chi_{2,2}(\tau,\xi) = \sum_{n=0}^{N-1}\sum_{n'=0}^{N-1}\sum_{m=0}^{M-1}\sum_{m'=0}^{M-1}\left\{\left(T_b-\left|nT_2-n'T_2-\tau\right|\right)d_{n,m}d_{n',m'}^*\mathrm{e}^{j2\pi\Delta f(n'm'T_2-nmT_2+m'\tau)}\mathrm{e}^{j\pi F(T_b+nT_2+n'T_2+\tau)}\mathrm{sinc}\left[\left(m\Delta f-m'\Delta f+\xi\right)\left(T_b-\left|nT_2-n'T_2-\tau\right|\right)\right]\right\} \quad (14)$$

$$\cdot\mathrm{e}^{j2\pi\xi T_g}, \quad \left|\left(n-n'\right)T_2-\tau\right| \le T_b$$

Equation (14) indicates that expectation value of the OFDM data segment's AF depends on the cross-correlation function $\mathscr{E}[d_{n,m}d_{n',m'}^*]$. When $n \ne n'$ or $m \ne m'$, $d_{n,m}$ and $d_{n',m'}$ represent modulation data in different symbols or subcarriers, which are independent according to the hypothesis above, hence the cross-correlation function equals zero. $\mathscr{E}[d_{n,m}d_{n',m'}^*]$ will only have a nonzero value in case $n = n'$ and $m = m'$. This results in the following expression.

$$\mathscr{E}\left[d_{n,m}d_{n',m'}^*\right] = \begin{cases}\left|d_{n,m}\right|^2, & n = n' \text{ and } m = m' \\ 0, & \text{others}\end{cases} \quad (15)$$

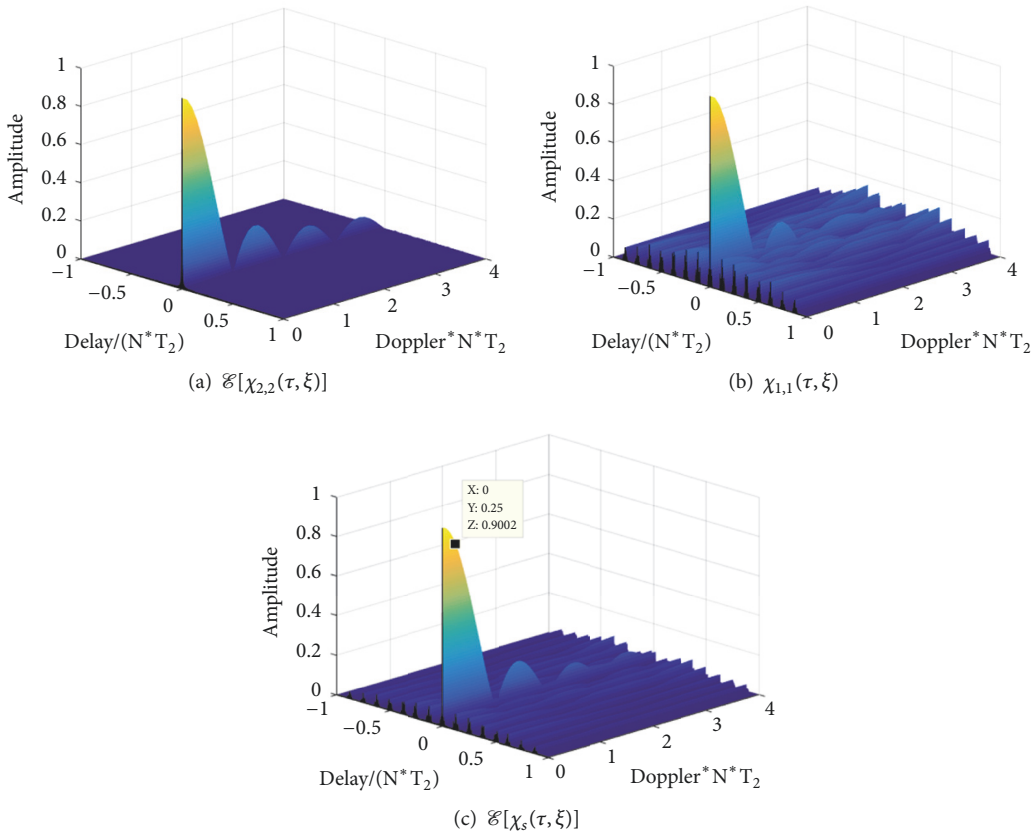

(a) $\mathscr{E}[\chi_{2,2}(\tau,\xi)]$ (b) $\chi_{1,1}(\tau,\xi)$

(c) $\mathscr{E}[\chi_s(\tau,\xi)]$

FIGURE 2: Ambiguity function of TDS-OFDM RadCom signal (M=128, N=8, K=32).

Specifically, when QAM modulation is adopted, the right side of (15) should be $\mathscr{E}(|d_{n,m}|^2)$. For simplicity, PSK modulation is assumed here. combining (14) and (15), the expectation of AF of $s_2(t)$ can be finally expressed as follows.

$$\mathscr{E}\left[\chi_{2,2}(\tau,\xi)\right] = (T_b - |\tau|)\,\mathrm{sinc}\left[\xi\left(T_b - |\tau|\right)\right] \cdot e^{j2\pi\xi T_g} \sum_{n=0}^{N-1}\sum_{m=0}^{M-1}\left\{|d_{n,m}|^2 \cdot e^{j2\pi m\Delta f\tau}\, e^{j\pi\xi(T_b+2nT_2+\tau)}\right\}, \quad -T_b < \tau \le T_b \tag{16}$$

Equation (16) indicates that $\mathscr{E}[\chi_{2,2}(\tau,\xi)]$ is nonzero only within the delay range of a single symbol, where the rest are all zero. Figure 2(a) shows a function graph of the OFDM data segment's AF, which is generally ideally thumbtack-typed.

3.3. Ambiguity Function of TS-String. According to the definition, substituting (2) into (4), AF of TS-string is as follows.

$$\chi_{1,1}(\tau,\xi) = \sum_{n=0}^{N-1}\sum_{n'=0}^{N-1}\sum_{k=0}^{K-1}\sum_{k'=0}^{K-1}\left\{c_{n,k}c_{n',k'}^{*}\int_{-\infty}^{+\infty} e^{j2\pi\xi t}\,\mathrm{rect}\left(\frac{t-kT_1-nT_2}{T_1}\right)\mathrm{rect}\left(\frac{t-k'T_1-n'T_2-\tau}{T_1}\right)dt\right\} \tag{17}$$

Similar to the deriving process of (10) to (13), we can derive the integral term in (17); the final expression of TS-string's AF is presented as

$$\chi_{1,1}(\tau,\xi) = \sum_{n=0}^{N-1}\sum_{n'=0}^{N-1}\sum_{k=0}^{K-1}\sum_{k'=0}^{K-1}\left\{c_{n,k}c_{n',k'}^{*}\left(T_1 - \left|\Delta kT_1 + \Delta nT_2 - \tau\right|\right)e^{j\pi\xi[(k+k'+1)T_1+(n+n')T_2+\tau]}\,\mathrm{sinc}\left[\xi\left(T_1 - \left|\Delta kT_1 + \Delta nT_2 - \tau\right|\right)\right]\right\}, \quad \left|\Delta kT_1 + \Delta nT_2 - \tau\right| \le T_1 \tag{18}$$

where $\Delta k = k - k'$ and $\Delta n = n - n'$. And the value range of τ is determined by the value of Δk and Δn. Let $\tau = 0$; hence $\Delta k = 0$ and $\Delta n = 0$. Therefore we can get the zero-delay cut of AF.

$$\chi_{1,1}(0,\xi) = T_1 \sum_{n=0}^{N-1} \sum_{k=0}^{K-1} \left\{ \left| c_{n,k} \right|^2 \operatorname{sinc}(\xi T_1) \, e^{j\pi\xi[(2k+1)T_1 + 2nT_2]} \right\} \tag{19}$$

As the amplitude of $c_{n,k}$ is constant, (19) indicates that Doppler tolerance of TS-string is independent of the TS. Therefore, the impact on Doppler tolerance is out of consideration when designing TS-string. Moreover, assigning $\tau = \Delta k T_1 + \Delta n T_2$ and letting $\xi = 0$, we can get the range autocorrelation sequence of TS-string.

$$\chi_{1,1}(\Delta k + M\Delta n) = T_1 \sum_{n=0}^{N-1} \sum_{n'=0}^{N-1} \sum_{k=0}^{K-1} \sum_{k'=0}^{K-1} c_{n,k} c_{n',k'}^{*} \tag{20}$$

As shown in (20), when $\Delta n = 0$, $\chi_{1,1}$ equals the sum of N ACF of TS in the range of $|\tau| < T_2$; when $\Delta n > 0$, $\chi_{1,1}$ equals the sum of cross-correlation function of different TS in the range of $|\tau| > T_2$. Thus, as shown in Figure 2(b), grating lobes are found on the AF along the delay axis. To reduce PSL, training sequences should be designed to ensure both good autocorrelation and cross-correlation.

Substituting (16) and (18) into (6), AF of TDS-OFDM RadCom signal is obtained as shown in Figure 2(c), whose mathematical expression is no more described here. As can be seen from Figure 2, AF sidelobes of TDS-OFDM RadCom signal are mainly caused by TS-string, and thus it is necessary to optimize it. And on the zero-delay cut of AF, the function value is about 0.9 at the position of normalized Doppler shift of ξ=0.25, which indicates that its Doppler tolerance is consistent with conventional OFDM RadCom signal [19].

4. Design of Training Sequences

PSL of radar signal is an important factor affecting radar target detection. In this section, PSL of average ACF of TDS-OFDM signals, denoted as PSL_0, is used as one of the objective functions

$$\mathrm{PSL}_0 = -20 \lg \max_{k \neq 0} \left| \mathscr{E}\left[\chi_s(k) \right] \right| \tag{21}$$

where $\mathscr{E}[|\chi_s(k)|]$ is the expectation of autocorrelation sequence of TDS-OFDM RadCom signal. To reduce the sidelobes of OFDM data blocks within the delay range of T_b, Hamming window function was used in the autocorrelation operation.

On the other hand, to realize robust communication synchronization and channel estimation, TS itself should be well autocorrelated. Let $r_{n,n}(k)$ represent the aperiodic autocorrelation sequence of nth TS.

$$r_{n,n}(k) = \sum_{m=k}^{K-1} c_{n,m} c_{n,m-k}^{*} \tag{22}$$

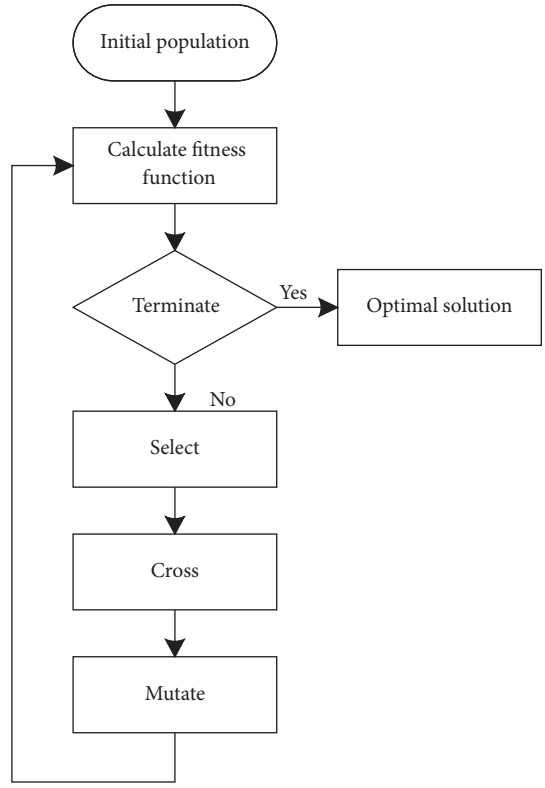

Figure 3: Flow chart of GA.

And the other objective function is the maximal peak sidelobe of N TS.

$$\mathrm{PSL}_{\mathrm{TS}} = -20 \lg \max_{\substack{k=1,\cdots,K-1 \\ n=0,\cdots,N-1}} \left| r_{n,n}(k) \right| \tag{23}$$

Thus, the final optimizing criterion is minimizing the weighted sum of average peak sidelobe of TDS-OFDM signal and maximal peak sidelobe of TS, which is presented as the following fitness function:

$$E = -\left(\omega_1 \mathrm{PSL}_0 + \omega_2 \mathrm{PSL}_{\mathrm{TS}} \right) \tag{24}$$

where ω_1 and ω_2 are, respectively, the weights of two costs, and $\omega_1 + \omega_2 = 1$. As (24) involves a nonlinear multivariable optimization problem, genetic algorithm (GA) is utilized for designing TS. The flow chart of GA is depicted in Figure 3, and the algorithm flow is as follows.

Step 1. Initialize the population $\mathbf{S}^{(0)}$ with numbers randomly produced by 0 and 1. For example, if there are two TS in a TS-string, and each TS contains four code elements, the population size is four. Thus, $\mathbf{S}^{(0)}$ can be represented as

$$\mathbf{S}^{(0)} = \pi \begin{bmatrix} 1 & 0 & 1 & 1 & 0 & 0 & 1 & 0 \\ 0 & 1 & 0 & 1 & 1 & 1 & 0 & 0 \\ 1 & 1 & 0 & 0 & 0 & 1 & 1 & 1 \\ 0 & 1 & 0 & 1 & 1 & 1 & 0 & 0 \end{bmatrix} \tag{25}$$

where each row of $\mathbf{S}^{(0)}$ represents an individual.

Table 1: Parameters of TDS-OFDM signal.

Parameters	Value
Number of OFDM symbols (N)	4
TS length (K)	63
Number of sub-carriers (M)	256
Bandwidth (B)	20MHz
Duration of an OFDM data block (T_b)	12.8μs
Duration of guard interval (T_g)	3.15μs
Pulse width	63.8μs
Time-bandwidth product	1276

Step 2. Calculate fitness value according to the fitness function represented by (24), and adjust the weights ω_1 and ω_2 to balance PSL_0 and $\mathrm{PSL}_{\mathrm{TS}}$.

Step 3 (select operators). According to the individual fitness, select superior individuals and eliminate inferior individuals by roulette selection.

Step 4 (cross operators). Recombine individuals with one-point crossover method.

Step 5 (mutate operators). Mutate individual gene values with 0.1 mutation probability.

Step 6 (terminate). When the iterations number reaches its maximum, the genetic algorithm completes and the optimization operation can be terminated. If the termination condition is not satisfied, go back to Step 2 to continue the optimization process.

Besides, the time complexity of GA is linearly increasing with iterative times and input size. When using the termination strategy above, the time complexity of GA can be approximately described as $O(G_{\max}NK)$, where $G_{\max}$ is the maximum iterative times. N and K represent the amount and the length of TS, respectively.

5. Simulation Result and Analysis

In the following simulations, GA parameters are as follows: the number of individuals is 100, maximum number of generations is 120, generation gap is 0.9, and weight ω_1=0.8.

5.1. Algorithm Simulation. We first optimize the TDS-OFDM RadCom signal with high time-bandwidth product whose parameters are shown in Table 1. The iterative process is shown in Figure 4. As the number of iterations increases, fitness of the population decreases gradually. ACF of the designed TS is shown in Figure 5 which contains 4 curves, and each curve represents a TS of the TS-string. As shown in Figure 5, maximal PSL of all training sequences is 15.99 dB, enabling the signal to achieve robust communication synchronization and channel estimation performance.

By using the designed TS-string, average ACF of TDS-OFDM signal is shown in Figure 6. As shown in the figure,

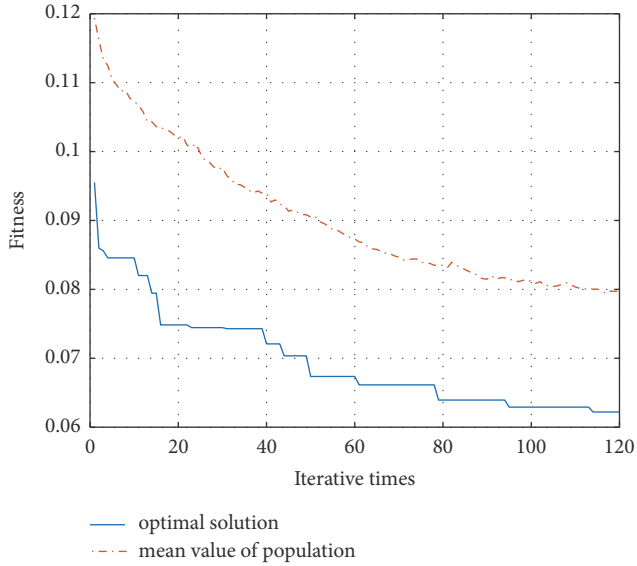

Figure 4: Fitness change of GA algorithm.

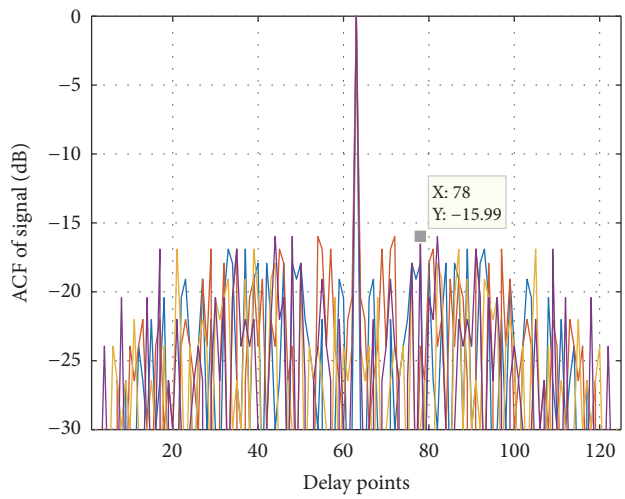

Figure 5: ACF of 4 training sequences.

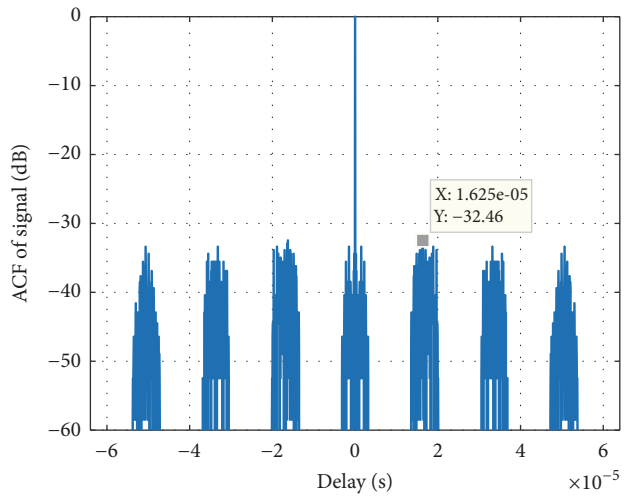

Figure 6: Average ACF of TDS-OFDM signal.

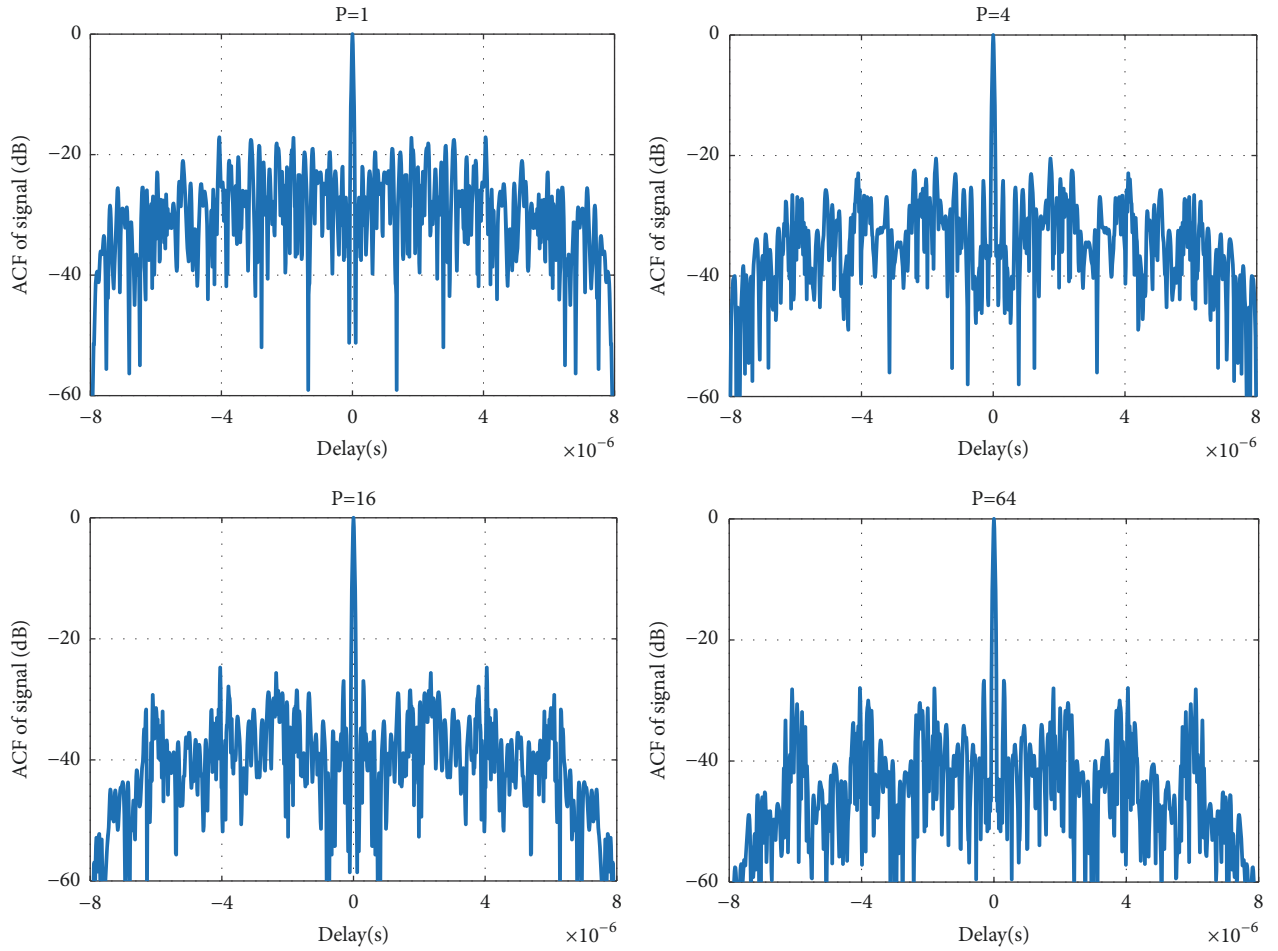

Figure 7: ACF of TDS-OFDM signal (MN=128).

PSL_0 of the signal is 32.46 dB, which means the designed signal on average is able to detect weak targets.

5.2. Analysis of Impact of Correlation Noise. In the ACF of TDS-OFDM signals, there are accompanying noise-like floors which are caused by the random OFDM data. Therefore, the instantaneous PSL of random TDS-OFDM signal will be lower than PSL_0. The noise-like effect of the random components in the transmitted signal is described as correlation noise in [20]. In the presence of correlation noise, PSL is reduced as

$$\mathrm{PSL} = \frac{\mathrm{PSL}_0 \, (\mathrm{S/N})_0}{\mathrm{PSL}_0 + (\mathrm{S/N})_0} \tag{26}$$

where $(S/N)_0$ represents the power ratio of signal to correlation noise. For one OFDM symbol, $(S/N)_0$ equals the subcarrier number M [18]. Furthermore, after the use of N symbols within each pulse and coherent integration of P pulses, $(S/N)_0$ becomes

$$\left(\frac{\mathrm{S}}{\mathrm{N}}\right)_0 = MNP \tag{27}$$

where MN is also the time-bandwidth product of OFDM data blocks. Equations (26) and (27) indicate that by increasing the number of time-bandwidth product or phase-coherent accumulation pulse, PSL will gradually approach PSL_0.

To verify this analysis, in this subsection, after phase-coherent accumulation of P pulses, ACF of designed TDS-OFDM signals with low and high time-bandwidth product were simulated, respectively, and P equals 1, 4, 16, and 64.

Figure 7 shows ACF of TDS-OFDM RadCom signal with low time-bandwidth product, whose parameters are N=4, M=32, K=8, B=20MHz, and PSL_0=28.52. As shown in the figure, correlation noise leads to a significant fluctuation of ACF, and PSL of a single pulse is only about 20dB. With the growth of accumulation pulse number, the fluctuation of ACF decreases gradually. When P is 64, PSL is about 28dB, which is very close to PSL_0.

Figure 8 shows the ACF of TDS-OFDM RadCom signal with high time-bandwidth product, whose parameters are the same as Table 1 (PSL_0=32.46dB). As the time-bandwidth product is high, the fluctuation of sidelobe decreases relatively. PSL reaches about 32dB after phase-coherent accumulation of just 16 pulses. In addition, by comparing Figures 6 and 8, it is obvious that, with the growth of pulse number of coherent accumulation, ACF of the TDS-OFDM signal approaches its expectation gradually.

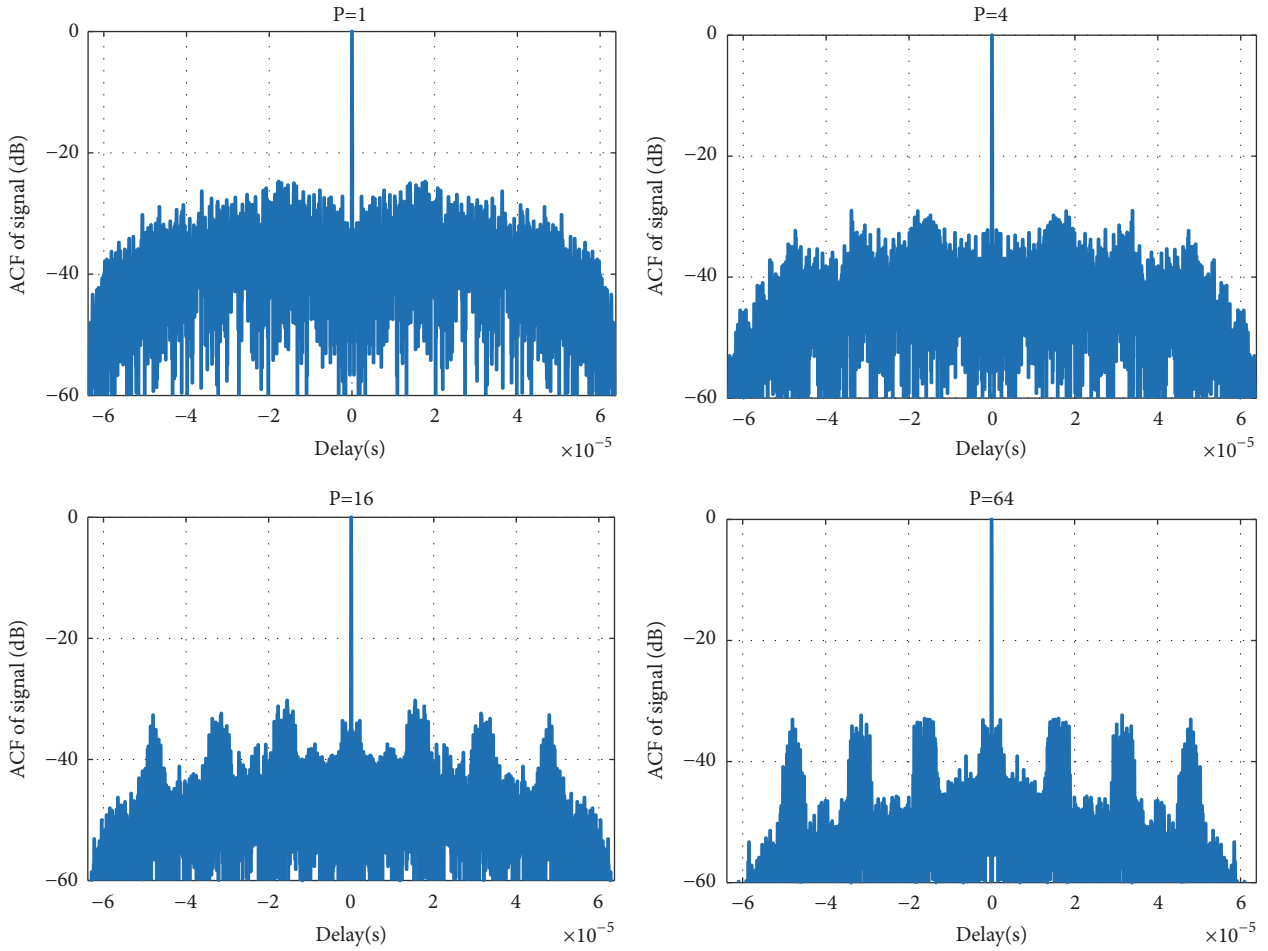

Figure 8: ACF of TDS-OFDM signal (MN=1024).

This simulation indicates that, as the technology of phase-coherent accumulation is generally used in modern radar, even if the time-bandwidth product of the signal is not high enough, ACF can also approach its expectation by using more pulses in phase-coherent accumulation, which means the signal design method based on optimizing average PSL is effective.

Furthermore, simulation of range ACF of CP-OFDM RadCom signal after phase-coherent accumulation of 16 pulses is also conducted in the same condition in Table 1. As shown in Figure 9, the CP sidelobes are about 15dB and pilot sidelobes of different sizes are also found in ACF of CP-OFDM RadCom signal. By comparing Figures 8 and 9, we can find that the autocorrelation performance of optimized TDS-OFDM RadCom signal is much better than that of CP-OFDM RadCom signal.

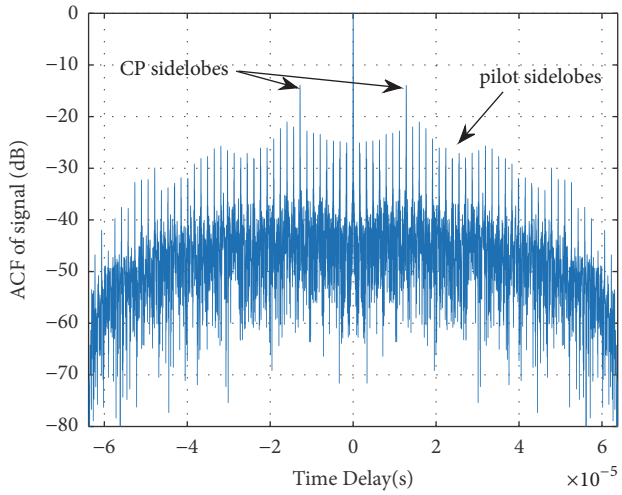

Figure 9: ACF of CP-OFDM signal (MN=1024, P=16).

5.3. Performance Comparison. As pseudorandom noise (PN) sequences are usually used in conventional TDS-OFDM communication signal, in this subsection, we compare the optimized sequence with m sequence and Gold sequence about the performance of PSL_{TS} and PSL_0. The data of three different sequence lengths is shown in Table 2, which is obtained in a random experiment. The table shows that PSL_{TS} of m sequence is the highest while PSL_0 is low, making it only suitable for communication. On the contrary, PSL_0 of Gold sequence is higher because of the good cross-correlation,

Table 2: Performance comparison of different TS.

Length	Sequence	PSL_{TS} (dB)	PSL_0 (dB)
31	m sequence	14.26	23.38
	Gold sequence	10.74	27.72
	optimized sequence	14.26	30.74
63	m sequence	15.99	17.36
	Gold sequence	10.41	21.22
	optimized sequence	15.99	32.46
127	m sequence	19.80	11.91
	Gold sequence	15.63	19.66
	optimized sequence	17.47	34.47

Table 3: Elapsed time of GA (N=4).

Length of TS	20	40	60	80	100	120
Elapsed time (sec)	6.79	7.62	8.02	9.34	9.72	10.1

but PSL_{TS} is the lowest. In contrast, the optimized sequence with different lengths is superior in both two properties, demonstrating the effectiveness of optimization algorithm. Furthermore, the performance of optimized sequence is relatively improved with the increase of sequence length. Because the increase of length leads to higher freedom of designing. In addition, the lengths of m sequence and Gold sequence cannot meet the needs of complex wireless transmission environment as their lengths are restricted by $2^K - 1$, while our method is not limited by sequence length which has greater flexibility.

The elapsed time of the GA program is shown in Table 3. The specification of computer is as follows: CPU is quad core at 2.4 GHz, 8GB RAM, operating system is Windows 10, and platform is MATLAB 2016a. As the optimization method is independent of communication data, TS-string should be renewed only when the signal's parameters change. Therefore, RadCom system does not demand much of the real-time characteristics, which means GA can almost meet the requirement of RadCom system in time complexity.

6. Conclusion

To address the problem of CP and pilot sidelobes in conventional CP-OFDM RadCom signal, a novel RadCom signal based on TDS-OFDM is proposed in this paper. AF of proposed signal was analyzed in detail. And then, TS are optimized to suppress PSL of TDS-OFDM signal and maintain the autocorrelation properties of TS simultaneously, thus achieving good performance in both radar and communication. Although, the TS and the OFDM data block cause mutual interference to each other, thus more calculation has to be costed to achieve reliable time-domain channel estimation and frequency-domain data detection in TDS-OFDM systems. Generally, considering the importance of autocorrelation of the signal to radar target detection, TDS-OFDM is more appropriate than CP-OFDM for the RadCom system.

Data Availability

The data used to support the findings of this study are available from the corresponding author upon request.

Conflicts of Interest

The authors declare that they have no conflicts of interest.

References

[1] P. Kumari, J. Choi, N. Gonzalez-Prelcic, and R. W. Heath, "IEEE 802.11ad-based radar: an approach to joint vehicular communication-radar system," *IEEE Transactions on Vehicular Technology*, vol. 67, no. 4, pp. 3012–3027, 2018.

[2] J. Moghaddasi and K. Wu, "Multifunctional transceiver for future radar sensing and radio communicating data-fusion platform," *IEEE Access*, p. 1, 2016.

[3] C. Sturm and W. Wiesbeck, "Waveform design and signal processing aspects for fusion of wireless communications and radar sensing," *Proceedings of the IEEE*, vol. 99, no. 7, pp. 1236–1259, 2011.

[4] G. C. Tavik and I. D. Olin, "The advanced multifunction RF concept (AMRFC) test bed," *IEEE Transactions on Microwave Theory and Techniques*, vol. 53, no. 3, pp. 1009–1020, 2005.

[5] N. Levanon and E. Mozeson, "Multicarrier radar signal—Pulse train and CW," *IEEE Transactions on Aerospace and Electronic Systems*, vol. 38, no. 2, pp. 707–720, 2002.

[6] T. Zhang and X. G. Xia, "OFDM synthetic aperture radar imaging with sufficient cyclic prefix," *IEEE Transactions on Geoscience and Remote Sensing*, vol. 53, no. 1, pp. 394–404, 2015.

[7] S. Sen, "PAPR-constrained pareto-optimal waveform design for OFDM-STAP Radar," *IEEE Transactions on Geoscience and Remote Sensing*, vol. 52, no. 6, pp. 3658–3669, 2014 (Danish).

[8] Y. Liu, G. Liao, Z. Yang, and J. Xu, "Multiobjective optimal waveform design for OFDM integrated radar and communication systems," *Signal Processing*, vol. 141, pp. 331–342, 2017.

[9] Y. Liu, G. Liao, Z. Yang, and J. Xu, "Design of integrated radar and communication system based on MIMO-OFDM waveform," *Journal of Systems Engineering and Electronics*, vol. 28, no. 4, pp. 669–680, 2017.

[10] Y. Liu, G. Liao, J. Xu, Z. Yang, and Y. Zhang, "Adaptive OFDM Integrated Radar and Communications Waveform Design Based on Information Theory," *IEEE Communications Letters*, vol. 21, no. 10, pp. 2174–2177, 2017.

[11] S. H. Dokhanchi, M. R. Shankar, T. Stifter, and B. Ottersten, "OFDM-based automotive joint radar-communication system," in *Proceedings of the 2018 IEEE Radar Conference (RadarConf18)*, pp. 0902–0907, Oklahoma City, OK, April 2018.

[12] Y. Zhou, H. Zhou, F. Zhou, Y. Wu, and V. C. Leung, "Resource allocation for a wireless powered integrated radar and communication system," *IEEE Wireless Communications Letters*, vol. 8, no. 1, pp. 253–256, 2019.

[13] X. Wan, Z. Zhao, D. Zhang, and Q. Shao, "HF passive bistatic radar based on DRM illuminators," in *Proceedings of the IEEE CIE International Conference on Radar*, vol. 1, IEEE, October 2011.

[14] Z. Zhao, X. Wan, D. Zhang, and F. Cheng, "An experimental study of HF passive bistatic radar via hybrid sky-surface wave mode," *IEEE Transactions on Antennas and Propagation*, vol. 61, no. 1, pp. 415–424, 2013.

[15] W. Zhang, Y. Guan, W. Liang, D. He, F. Ju, and J. Sun, "An introduction of the chinese DTTB standard and analysis of the PN595 working modes," *IEEE Transactions on Broadcasting*, vol. 53, no. 1, pp. 8–13, 2007.

[16] D. Linglong, W. Zhaocheng, and Y. Zhixing, "Compressive sensing based time domain synchronous OFDM transmission for vehicular communications," *IEEE Journal on Selected Areas in Communications*, vol. 31, no. 9, pp. 460–469, 2013.

[17] Z. Gao, C. Zhang, Z. Wang, and S. Chen, "Priori-information aided iterative hard threshold: a low-complexity high-accuracy compressive sensing based channel estimation for TDS-OFDM," *IEEE Transactions on Wireless Communications*, vol. 14, no. 1, pp. 242–251, 2015.

[18] R. F. Tigrek, W. J. A. De Heij, and P. Van Genderen, "OFDM signals as the radar waveform to solve doppler ambiguity," *IEEE Transactions on Aerospace and Electronic Systems*, vol. 48, no. 1, pp. 130–143, 2012.

[19] G. E. A. Franken, H. Nikookar, and P. Van Genderen, "Doppler tolerance of OFDM-coded radar signals," in *Proceedings of the 3rd European Radar Conference*, IEEE, September 2006.

[20] S. R. J. Axelsson, "Noise radar using random phase and frequency modulation," *IEEE Transactions on Geoscience and Remote Sensing*, vol. 42, no. 11, pp. 2370–2384, 2004.